# Room temperature ageing of Al–Ni–RE (RE = La, Gd, Er) metallic glasses

Rina Sahu,[a] A.K. Gangopadhyay,[b] K.F. Kelton,[b] S. Chatterjee[c] and K.L. Sahoo[a,*]

[a]National Metallurgical Laboratory, Jamshedpur 831007, India
[b]Department of Physics, One Brokings Drive, Washington University in St. Louis, MO 63130, USA
[c]Department of Metallurgical and Materials Engineering, Bengal Engineering and Science University, Shibpur, Howrah 711103, India

The effect of long-term ageing of Al–TM–RE (TM = Ni, Ag, Cu; RE = rare earth) amorphous alloys under ambient conditions, and at a slightly elevated temperature (100 °C), has been studied. The phase evolution and devitrification kinetics were studied using differential scanning calorimetry, X-ray diffraction and transmission electron microscopy techniques. Partial crystallization was observed in $Al_{89}Ni_6La_5$, $Al_{87}Ni_6La_7$, $Al_{87}Ni_5(Ag/Cu)_1La_7$ alloys after several years under ambient conditions (20–50 °C), and in $Al_{88}Ni_4La_8$, $Al_{88}Ni_4Gd_2Er_6$ and $Al_{88}Ni_4Er_8$ alloys following a 90 h anneal at 100 °C.
© 2009 Acta Materialia Inc. Published by Elsevier Ltd. All rights reserved.

Keywords: Al–Ni–RE amorphous alloys; Room temperature ageing; Activation energy; Differential scanning calorimetry

Glasses are supercooled liquids, frozen into a metastable state and kinetically constrained from transforming into the thermodynamically stable crystalline state. Glasses occur in a wide variety of materials, including silicates (common window glass), polymers and metallic alloys, and are extensively used for applications in everyday life. A natural concern for any metastable material is whether the transformation to the stable state is possible over practical timescales under the operating environment. A case in point is the popular belief that since it is a supercooled liquid, common window glass flows and deforms over millennium timescales, which has recently been proven to be a myth [1]. However, the more practical issues of partial crystallization of most metallic glasses over long timescales and associated changes in physical properties have not been reported thus far. In this paper, we present the results of such studies for some Al-based metallic glasses (Al–Ni–RE, where RE = rare earth) at room and intermediate temperatures. Surprisingly, a significant amount of crystallization was observed over practical timescales of many years at ambient temperatures in tropical climates (reaching up to 50 °C in summer), or over a few days at a moderate temperature of 100 °C.

Al-based metallic glasses have received significant attention since their discovery [2,3] due to their attractive physical properties. An enormous amount of work has been devoted towards understanding the structure [4], crystallization kinetics [5,6] and glass-forming abilities [7,8] of these materials. The amorphous alloys form over a wide concentration range of Al, depending on the transition metal and RE element [2]. The transformation of the amorphous alloys to the fully crystalline state follows composition-dependent pathways [9]. The primary crystallization products are usually a nanocrystalline face-centered cubic (fcc) Al phase, a body-centered cubic (bcc) metastable phase, or a mixture of these phases, depending on the alloy composition. The precise devitrification mechanism is still debated after many years of extensive research [10–12]. Chemical phase separation prior to crystallization [12], growth on pre-existing nuclei/clusters [5,13] or on defects in the amorphous matrix [10] have been suggested. Although the as-quenched alloys appear to be amorphous from conventional X-ray diffraction (XRD) and transmission electron microscopy (TEM) studies, the existence of medium-range order and chemical concentration fluctuations on the nanometer scale have been observed in some cases from recent small-angle neutron scattering [14] and three-dimensional atom tomography experiments [13]. This nanoscale inhomogeneity raises the possibility that the amorphous phase is weakly metastable, and therefore

---

* Corresponding author; e-mail addresses: klsahoo@gmail.com; klsah@nmlindia.org

may transform with ageing at moderate, or even at ambient temperatures.

To investigate this, a series of amorphous Al–Ni–RE alloys were studied several years after their preparation by two different groups. The results presented here are for alloys containing 87–89 at.% Al, 4–6 at.% Ni and 5–8 at.% RE (Table 1). Although many compositions were studied, only those that showed an ageing effect are discussed here. The alloys prepared in India and the USA are designated as alloy sets A and B, respectively. Both sets of alloys were prepared by arc-melting 5 N/4 N pure elements in a Ti-gettered Ar atmosphere, followed by single-roller quenching, at a linear wheel speed of 40 m s$^{-1}$ for set A and 55 m s$^{-1}$ for set B alloys. Amorphous ribbons in set A are ~25 μm thick, compared to ~20 μm for the set B alloys. The alloy set A was kept in a sealed container under ambient tropical conditions (high humidity and temperatures, approaching 50 °C during the summer months) for a period of up to 5 years. The alloy set B was kept in a more controlled and less humid atmosphere, with the temperature maintained around 15–25 °C over about 10 years.

The crystallization temperature and crystallization enthalpy were measured by differential scanning calorimetry (DSC). Before each measurement, the calorimeter was calibrated using pure In and Zn standards, giving an accuracy of ±0.3 K for temperature and ±0.02 mW for heat flow measurements. The amorphous/crystalline nature of the as-quenched, aged and annealed samples was determined by XRD and TEM. The TEM samples were prepared by a twin-jet polisher in an electrolyte of 2:1 $CH_3OH$ and $HNO_3$ operated at 12 V and −40 °C. For low-temperature ageing, the samples were sealed in a quartz tube under vacuum and annealed for 90 h at 100 °C.
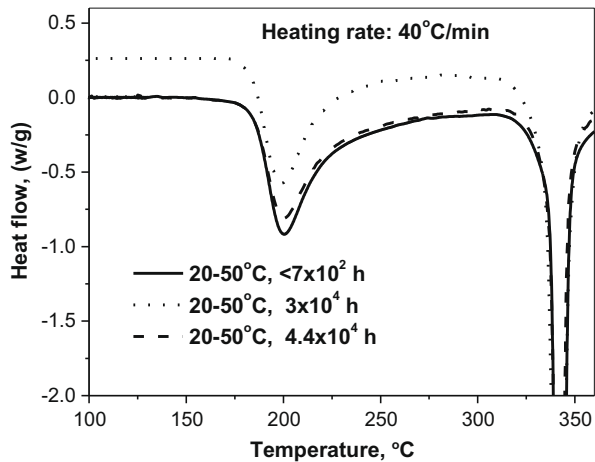
The XRD patterns of all as-quenched ribbons (not shown) showed featureless broad diffraction patterns, typical of amorphous solids. Figure 1 shows continuous heating DSC curves for an as-quenched $Al_{89}Ni_6La_5$ amorphous alloy and after room temperature ageing for different times. The alloy shows two stages of crystallization: the first crystallization corresponds to the precipitation of fcc Al and the second to $Al_3Ni$ and $Al_{11}La_3$ [9]. A comparison of the primary crystallization enthalpy (δH) of the first stage shows a significant decrease from an initial value of 43 J g$^{-1}$ for the as-quenched alloy to 34 J g$^{-1}$ after $3 \times 10^4$ h and 29.6 J g$^{-1}$ after $4.4 \times 10^4$ h at room temperature (Table 1), approximately a 31% decrease after 5 years. The corresponding crystallization onset and peak temperatures show little or no changes. The changes in the second and third crystallization enthalpies are much smaller, and therefore are not reported. The change in δH clearly indicates significant partial crystallization of the amorphous alloy at ambient temperature (20–50 °C). To further confirm this, TEM bright-field (BF) images and selected-area diffraction (SAD) patterns were obtained from several different parts of the as-quenched and $4.4 \times 10^4$ h aged samples; representative micrographs are shown in Figure 2a and b, respectively. Compared to the fully amorphous state of the as-quenched sample, the aged sample shows a significant quantity of 15–35 nm diameter fcc Al crystals.

When Al is replaced by more La ($Al_{87}Ni_6La_7$), the crystallization temperature increased to 250.6 °C, indicating a higher stability compared to $Al_{89}Ni_6La_5$. Consistent with this observation, the room temperature ageing of this alloy is also smaller (a 10.6% decrease in δH after 5 years, see Table 1). The TEM images (not shown) indicated that the as-quenched amorphous alloy evolved into a partially crystalline state after room temperature ageing, containing the same bcc metastable phase (10–20 nm diameter), which appears during the primary crystallization of this alloy at higher temperatures [9]. The transformed volume fraction and the number density of crystallites are significantly smaller than are observed in the aged $Al_{89}Ni_6La_5$ alloy, consistent with the DSC results. If, however, the Al and La concentrations are kept constant and 1 at.% Ni in $Al_{87}Ni_6La_7$ is replaced by Ag or Cu, the ambient temperature ageing effects are not significantly altered (Table 1). The first crystallization enthalpy decreased after 5 years by about

**Table 1.** The changes in the first crystallization enthalpy ($\delta H_1$, J g$^{-1}$), first crystallization peak temperature ($T_{xp1}$, °C), measured at 40 °C min$^{-1}$ for the set A alloys and 20 °C min$^{-1}$ for the set B alloys, for various alloys as a function of ageing temperature ($T_a$, °C) and time ($t_a$, h).
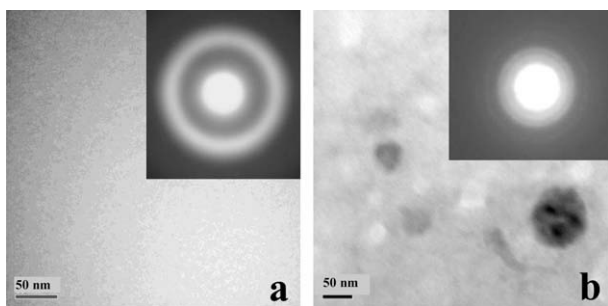
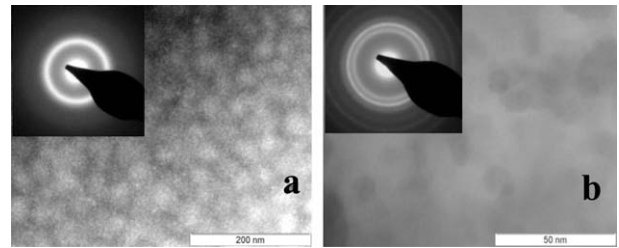| Alloy | Composition | $T_a$ | $t_a$ | $T_{xp1}$ | $\delta H_1$ |
|-------|-------------|-------|-------|-----------|--------------|
| Set A | $Al_{89}Ni_6La_5$ | 20–50 | $<7 \times 10^2$ | 200.4 | −43.0 |
| | | 20–50 | $3 \times 10^4$ | 198.5 | −34.0 |
| | | 20–50 | $4.4 \times 10^4$ | 199.4 | −29.6 |
| | $Al_{87}Ni_6La_7$ | 20–50 | $<7 \times 10^2$ | 262.4 | −26.4 |
| | | 20–50 | $4.4 \times 10^4$ | 262.8 | −23.6 |
| | $Al_{87}Ni_5Ag_1La_7$ | 20–50 | $<7 \times 10^2$ | 247.1 | −23.5 |
| | | 20–50 | $4.4 \times 10^4$ | 246.8 | −20.5 |
| | $Al_{87}Ni_5Cu_1La_7$ | 20–50 | $<7 \times 10^2$ | 254.8 | −22.8 |
| | | 20–50 | $4.4 \times 10^4$ | 254.6 | −20.6 |
| Set B | $Al_{88}Ni_4Er_8$ | 15–20 | $<10^2$ | 226.7 | −24.0 |
| | | 100 | 90 | 227.1 | −21.2 |
| | $Al_{88}Ni_4Er_6Gd_2$ | 15–20 | $<7 \times 10^2$ | 236.5 | −23.5 |
| | | 15–20 | $8.8 \times 10^4$ | 239.1 | −22.9 |
| | | 100 | 90 | 239.7 | −21.3 |
| | $Al_{88}Ni_4La_8$ | 15–20 | $<7 \times 10^2$ | 250.3 | −23.2 |
| | | 15–20 | $8.8 \times 10^4$ | 253.7 | −23.0 |
| | | 100 | 90 | 252.4 | −21.8 |

**Figure 1.** Continuous heating DSC curves of an $Al_{89}Ni_6La_5$ amorphous alloy soon after quenching and after room temperature ageing for various times. The dotted line is shifted vertically and the second crystallization peak is truncated for clarity.



**Figure 3.** The TEM images (BF) of $Al_{87}Ni_5Cu_1La_7$ amorphous alloy after ambient temperature (20–50 °C) ageing for $3 \times 10^4$ h (a) and $4.4 \times 10^4$ h (b). The insets show the corresponding SAD pattern.

crystallization enthalpy indeed showed a significant decrease after this ageing treatment by 6% for $Al_{88}Ni_4La_8$, 9.4% for $Al_{88}Ni_4Er_6Gd_2$ and 11.7% for $Al_{88}Ni_4Er_8$, which correlates with the decreasing average atomic radius of the RE atom. The XRD pattern of $Al_{88}Ni_4Er_8$ clearly showed fcc Al after ageing (figure not shown); no such clear signature was observed for the other two alloys. However, the TEM micrographs of $Al_{88}$-$Ni_4Er_6Gd_2$ and $Al_{88}Ni_4La_8$ after 100 °C (90 h) anneal showed nanocrystals (Fig. 4a and b, respectively). The volume of nanocrystals also decreased with increasing RE element radius, consistent with the DSC results. This reinforces the view that the concentration and the atomic radius of the RE element is the primary controlling factor in the ambient and intermediate temperature ageing of these alloys. This is understandable as crystal growth involves the rejection of the RE and TM atoms from the amorphous alloy, and hence the transformation will be controlled by the slowest diffusing atom (RE).

To clarify whether the room and intermediate temperature ageing of these alloys is consistent with the kinetics of the amorphous to crystalline transformation, an estimate of the activation energy ($E_a$) of this process was made for a few selective compositions using the standard Kissinger analysis [15]. Although a strict interpretation of $E_a$ from such analysis is unclear [6], this quantity does provide a measure of the temperature dependence of the overall transformation kinetics. However, to obtain a reliable estimate of $E_a$, one must pay careful attention to instrumental shifts in the DSC temperature calibration with increasing heating rates. The melting temperature (a first-order phase transition) of a standard material as a function of scan rate does not give a proper measure of the instrumental shift since

12.8% for Ag and 9.6% for Cu replacing Ni. This indicates that the type of transition metal atom plays much smaller role in the ambient temperature stability of these alloys. The microstructure of the $Al_{87}Ni_5Cu_1La_7$ alloy shows some interesting features (Fig. 3). The mottled structure in Figure 3a after $3 \times 10^4$ of ambient temperature ageing suggests a chemical phase separation in the amorphous matrix, similar to earlier reports in related alloys [12,13]. There is no evidence from the SAD pattern for the formation of nanocrystals as a result of this anneal (inset of Fig. 3a). However, the microstructure changes dramatically for longer ageing treatments. A $4.4 \times 10^4$ h treatment causes the mottled structure to evolve to an amorphous/nanocrystal composite (Fig. 3b).

Among the alloys in set B only $Al_{88}Ni_4La_8$ and $Al_{88}$-$Ni_4Er_6Gd_2$ showed a noticeable change (1 and 2.5%, respectively, see Table 1) over a decade ($8.8 \times 10^4$ h). To investigate this further, the alloys were annealed at 100 °C (90 h) under vacuum, which is much lower than the crystallization onset temperatures (Table 1). Another composition, $Al_{88}Ni_4Er_8$, containing a much smaller RE atom, was also included in this study from a freshly quenched sample (the decade-old sample was consumed in the earlier investigations). The primary
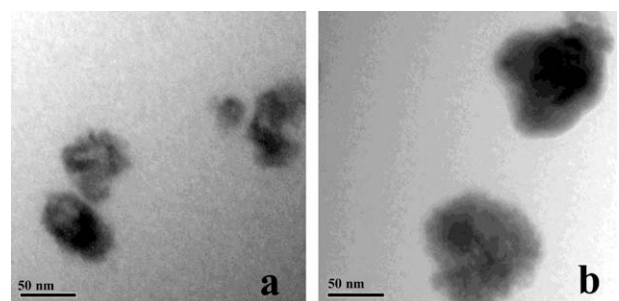


**Figure 2.** The TEM bright field images of $Al_{89}Ni_6La_5$ amorphous alloy in the as-quenched state ($<7 \times 10^2$ h) (a), and after room temperature ageing for $4.4 \times 10^4$ h at 20–50 °C (b). The insets show the corresponding SAD pattern.
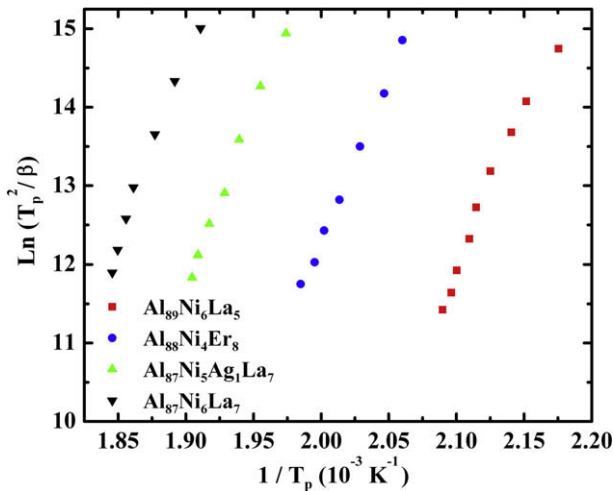


**Figure 4.** The TEM images (BF) of $Al_{88}Ni_4Gd_2Er_6$ (a) and $Al_{88}Ni_4La_8$ (b) alloys after 100 °C (90h) anneals.

**Figure 5.** Kissinger plots of Al–Ni–RE amorphous alloys for the primary crystallization event.

the phase transition itself has an intrinsic heating rate dependence. Instead, the ferromagnetic transition temperature (Curie temperature) of Ni, a second-order phase transition that is independent of the heating rate, was measured simultaneously and used for temperature correction. Taking the instrumental shift into account, the corrected Kissinger plots for the primary crystallization of freshly prepared $Al_{89}Ni_6La_5$, $Al_{88}Ni_4Er_8$, $Al_{87}Ni_6La_7$ and $Al_{87}Ni_5Ag_1La_7$ alloys are shown in Figure 5. The slopes of these plots give the $E_a$ values. However, it is quite clear that, instead of straight lines, the plots show considerable curvature, indicating a temperature-dependent $E_a$. A recent experimental result [16] indicated a change in the slope of the Kissinger plots ($E_a$) with heating rate, suggesting an increase in $E_a$ in the amorphous state below $T_g$ (low heating rate), compared to the supercooled state (above $T_g$). The present results, in contrast, indicate a higher value of $E_a$ in the supercooled state compared to the amorphous state.

Because the ambient temperature transformation took place in the amorphous state, approximate values of $E_a$ in the amorphous state were estimated from the slower heating rate data (5–40 °C min$^{-1}$). The $E_a$ values are $259 \pm 12$, $356 \pm 18$, $325 \pm 16$ and $343 \pm 18$ kJ mol$^{-1}$ for $Al_{89}Ni_6La_5$, $Al_{88}Ni_4Er_8$, $Al_{87}Ni_5Ag_1La_7$ and $Al_{87}Ni_6La_7$, respectively. Assuming the same activation energy at the ambient temperature of 50 °C, the transformation should be slowed down by a factor of exp($-E_a/RT_{x1}$)/exp($-E_a/RT_a$), where $T_{x1}$ is the first crystallization onset temperature, $T_a$ is the ageing temperature, and R is the molar gas constant. The estimated values of these factors are $1.6 \times 10^{11}$, $1.2 \times 10^{18}$, $7.5 \times 10^{18}$ and $1.2 \times 10^{21}$ for the $Al_{89}Ni_6La_5$, $Al_{88}Ni_4Er_8$, $Al_{87}Ni_5Ag_1La_7$ and $Al_{87}Ni_6La_7$, respectively. Therefore, no transformation is expected at 50 °C over the 5–10 year period (1.58–3.15 $\times 10^8$ s).

Based on the above analyses, the observed long-term ageing effect at ambient or slightly elevated temperatures for these Al-based amorphous alloys is surprising. Although the exact mechanism is not clear, a few possibilities can be highlighted. First, the ambient temperature $E_a$ may be much smaller than the higher-

temperature values. The curvature in the Kissinger plots (Fig. 5) is indicative of that. Interestingly, the diffusivity measurements in Zr-based alloys [17] showed a much higher diffusion coefficient (lower activation energy) in the amorphous state, compared to the extrapolated values from the supercooled liquid state. The authors suggested [17] that a change in cooperative dynamics in the supercooled state to single-particle dynamics in the amorphous state results in a lower effective $E_a$ in the amorphous state. Second, the quenched glass contains a larger free volume than the glass that is crystallized at higher temperatures. Structural relaxation during heating is expected to anneal out a significant amount of free volume before crystallization takes place. Since diffusivity increases exponentially with the amount of free volume [18], diffusivity is expected to be higher in the quenched glass than what is anticipated from a simple extrapolation of the higher-temperature data. Both of these factors are expected to underestimate the ambient temperature kinetics when high-temperature data are extrapolated. In addition to the thermal mechanisms, possible chemical effects associated with the higher-humidity environment for the set A alloys may also be a contributing factor for the enhanced transformation kinetics.

In conclusion, significant ambient temperature ageing effects have been observed in a number of Al-based amorphous alloys. Although the exact mechanism of the observed changes is not completely clear from this investigation, these long-term changes in the microstructure and their impact on physical properties need to be considered for future application of these, and perhaps other, metallic glasses.

[1] E.D. Zanotto, Am. J. Phys. 66 (1998) 392.
[2] A. Inoue, K. Ohtera, A.-P. Tsai, T. Masumoto, Jpn. J. Appl. Phys. 27 (1988) L280.
[3] Y. He, S.J. Poon, G.J. Shiflet, Science 241 (1988) 1640.
[4] O.N. Senkov, D.B. Miracle, Mater. Res. Bull. 36 (2001) 2183.
[5] D.R. Allen, J.C. Foley, J.H. Perepzko, Acta Mater. 46 (1998) 431.
[6] K.F. Kelton, Mater. Sci. Eng. A 226–228 (1997) 142.
[7] A.K. Gangopadhyay, K.F. Kelton, Philos. Mag. A 80 (2000) 1193.
[8] T. Egami, Mater. Sci. Eng. A 226–228 (1997) 261.
[9] K.L. Sahoo, M. Wollgarten, J. Haug, J. Banhart, Acta Mater. 53 (2005) 3861.
[10] I.A. Rauf, Appl. Phys. Lett. 93 (2008) 143101.
[11] A.K. Gangopadhyay, K.F. Kelton, Acta Mater. 48 (2000) 4035.
[12] T.K. Croat, A.K. Gangopadhyay, K.F. Kelton, Philos. Mag. A 82 (2002) 2483.
[13] B. Radiguet, D. Blavette, N. Wanderka, J. Banhart, K.L. Sahoo, Appl. Phys. Lett. 92 (2008) 103126, and references therein.
[14] T. Gloriant, D.H. Ping, K. Hono, A.L. Greer, M.D. Baro, Mater. Sci. Eng. A 304–306 (2001) 315.
[15] H.E. Kissinger, Anal. Chem. 29 (1957) 1702.
[16] N. Tian, M. Ohnuma, K. Hono, Scr. Mater. 53 (2005) 681.
[17] U. Geyer, W.L. Johnson, S. Schneider, Y. Qiu, T.A. Tombrello, M.-P. Macht, Appl. Phys. Lett. 69 (1996) 2492.
[18] F. Spaepen, D. Turnbull, Scr. Metall. 25 (1991) 1563.